



Lawrence Berkeley Laboratory

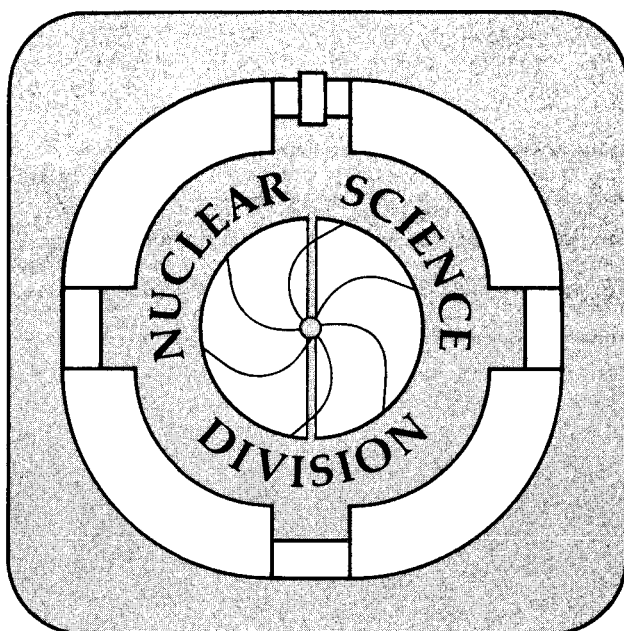
UNIVERSITY OF CALIFORNIA

Invited talk presented at the International Workshop on High Density Nuclear Matter, KEK, Tsukuba, Japan, September 18-21, 1990, and to be published in the Proceedings

Review of CERN Heavy-Ion Physics

J.W. Harris

December 1990



1 LOAN COPY 1
1 Circulates 1
1 for 2 weeks 1 Bldg. 50 Library.
Copy 2

LBL-30129

DISCLAIMER

This document was prepared as an account of work sponsored by the United States Government. While this document is believed to contain correct information, neither the United States Government nor any agency thereof, nor the Regents of the University of California, nor any of their employees, makes any warranty, express or implied, or assumes any legal responsibility for the accuracy, completeness, or usefulness of any information, apparatus, product, or process disclosed, or represents that its use would not infringe privately owned rights. Reference herein to any specific commercial product, process, or service by its trade name, trademark, manufacturer, or otherwise, does not necessarily constitute or imply its endorsement, recommendation, or favoring by the United States Government or any agency thereof, or the Regents of the University of California. The views and opinions of authors expressed herein do not necessarily state or reflect those of the United States Government or any agency thereof or the Regents of the University of California.

Invited talk presented at the International Workshop on High Density
Nuclear Matter, KEK, Tsukuba, Japan, September 18–21, 1990

Review of CERN Heavy-Ion Physics

John W. Harris
Nuclear Science Division
Lawrence Berkeley Laboratory
University of California
Berkeley, CA 94720

December 1990

This work was supported by the Director, Office of Energy Research,
Office of High Energy Nuclear Physics, Division of Nuclear Physics
of the U.S. Department of Energy under Contract No. DE-AC03-76SF00098.

Review of CERN Heavy-Ion Physics

John W. Harris
Nuclear Science Division, Lawrence Berkeley Laboratory,
University of California, Berkeley, California 94720 U.S.A.

I. Introduction

The primary motivation for studying nucleus-nucleus collisions at very high energies is the possibility of forming a quark-gluon plasma (QGP).¹ In these collisions energy and baryon densities are expected to increase and reach critical values where the quark constituents of the incident nucleons, bound in nuclei, form an extended volume of freely interacting quarks, antiquarks and gluons. Various signatures of the existence of a quark-gluon plasma in these collisions have been proposed: suppression of J/ψ production,² an enhancement in strange particle production,³ event-by-event fluctuations in the rapidity distributions of produced particles,⁴ observation of direct photons from the plasma⁵ and other observables.

The system is expected to evolve dynamically from a pure plasma or mixed phase (of plasma and hadronic matter) through expansion, cooling, hadronization and freeze-out. To be able to determine that a new, transient state of matter has been formed it is necessary not only to identify QGP signatures but also to determine the space-time evolution of the collision process. This requires an understanding of the microscopic structure of hadronic interactions, at the level of quarks and gluons, at high temperatures and high densities. In this talk I will describe the physical observables important for understanding the *dynamics of heavy-ion collisions* at high energies and the present status of experimental results covering these observables. I will then describe the various *signatures of QGP formation*, present experimental results and plausible interpretations of the results. This talk is not meant to be a comprehensive review, it is rather a summary of important background information, current outstanding problems, observations of particular interest and recent results on dynamics and signatures.

II. Collision Dynamics

Geometry

Information on the geometry of nucleus-nucleus collisions can be obtained from measured interaction cross sections, multiplicity distributions, rapidity distributions and the distributions of energy in the transverse and longitudinal directions in an event. The *interaction cross sections* are found to have a geometrical dependence on the radii of the colliding nuclei and are observed to be independent of incident energy for energies from 2 GeV/n to 200 GeV/n.^{6,7} The *transverse energy distributions* are observed to be impact parameter dependent and support a "clean-cut"

¹ see Proceedings of the Seventh International Conference on Ultra-Relativistic Nucleus-Nucleus Collisions, Nucl. Phys. A498 (1989), ed. G. Baym, P. Braun-Munzinger and S. Nagamiya.

² T. Matsui and H. Satz, Phys. Lett. B178 (1986) 416.

³ R. Hagedorn and J. Rafelski, Phys. Lett. 97B (1980) 180.

⁴ L. Van Hove, Z. Phys. C27 (1985) 135.

⁵ L.D. McLerran and T. Toimela, Phys. Rev. D31 (1985) 545.

⁶ A. Bamberger et al., Phys. Lett. B205 (1988) 583.

⁷ P. Barnes et al., Phys. Lett. B206 (1988) 146.

geometrical overlap of the colliding nuclei.^{8,9} For the nucleus-nucleus case of A_p projectile nucleons incident on A_T target nucleons the transverse energy distributions can be reproduced by an A_p -fold convolution of proton-nucleus collisions over the same range of impact parameters.^{8,9} An anti-correlation between the transverse energy and the energy remaining in the projectile and target fragmentation regions is observed which facilitates determination of the nuclear collision geometry.^{9,10,11} The first and second moments of *multiplicity distributions* for nucleus-nucleus collisions are well described by a superposition of proton-nucleus collisions,⁶ rather than a superposition of proton-proton collisions. *Rapidity distributions* of produced particles have been measured and are observed to peak at the rapidity of the center-of-mass of the geometrical overlap of the colliding nuclei.^{12,13,14} This information provides support for the important role that geometry plays in the dynamics of these collisions.

Stopping of Nuclear Matter

The production of a quark-gluon plasma in relativistic heavy ion collisions depends upon whether the energy density reached in the initial phase of the reaction is sufficiently high to initiate a phase transition. Creation of high energy densities requires large energy deposition from the longitudinal motion of the incident nuclei into excitation and transverse degrees of freedom. The degree to which nuclei can effectively redistribute the initial longitudinal motion into other degrees of freedom is referred to as the nuclear stopping power. Rapidity distributions of particles, primordial or produced, and transverse energy distributions provide information on the degree of stopping and the amount of thermalization in the collision process.

The peak positions of the *rapidity distributions of produced particles* are consistent with a simple geometrical overlap picture of the collision.^{13,14} The distributions are Gaussian in shape and are broader than expected for emission from an isotropic fireball.¹⁵ Whether the rapidity distributions represent a large degree of stopping in the Landau¹⁶ sense or partial stopping as predicted by string mechanisms in the Lund/FRITIOF model¹⁷ is still under intense investigation.¹⁸ Thus far, string models and variations^{15,19} of the Landau hydrodynamical model are able to predict the measured rapidity distributions of produced particles at CERN energies.

Rapidity distributions of the primordial protons, originally in the incident nuclei, provide direct information on the degree of stopping in these collisions. Identified proton rapidity distributions are not yet available from experiment for nucleus-nucleus collisions at CERN. The

⁸ A. Bamberger et al., Phys. Lett. B184 (1987) 271.

⁹ W. Heck et al., Z. Phys. C38 (1988) 19.

¹⁰ R. Albrecht et al., Phys. Lett. B199 (1987) 297.

¹¹ J.W. Harris et al., Nucl. Phys. A498 (1989) 133c.

¹² H. Stroebele et al., Z. Phys. C38 (1988) 89.

¹³ R. Albrecht et al., Phys. Lett. B202 (1988) 596.

¹⁴ L.M. Barbier et al., Phys. Rev. Lett. 60 (1988) 405.

¹⁵ H. von Gersdorf et al., Phys. Rev. C39 (1989) 1385.

¹⁶ L.D. Landau, Collected Papers, No. 88, Izv. Akad. Nauk, Ser. Fiz. 17 (1953) 51.

¹⁷ B. Andersson et al., Nucl. Phys. B281 (1987) 289; B. Nilsson-Almqvist and E. Stenlund, Comp. Phys. Commun. 43 (1987) 387.

¹⁸ see for example M. Prakash, Proceedings of the Workshop on Heavy Ion Physics at the AGS, Brookhaven National Laboratory Report BNL-44911, p.371.

¹⁹ J. Stachel and P. Braun-Munzinger, Phys. Lett. B216 (1989) 1.

NA35 Collaboration has measured rapidity distributions of "charge flow",²⁰ which can be associated with protons, by subtracting the distributions of all negative particles from those of positive particles to obtain the rapidity distributions of protons displayed in Fig. 1.²¹ The data are presented separately for peripheral and central collisions of 200 GeV/n S + S. The proton rapidity distribution from central collisions is flatter with significantly more yield at midrapidity than that from peripheral collisions. The central collision data are compared to predictions of two string models in Fig. 2. The rapidity distribution of protons from S + S central collisions exhibits considerably more stopping than predicted in the Lund/FRITIOF model which underpredicts the proton yield at rapidity $y = y_{cm} = 3$ as seen in Fig. 2a. Predictions of the VENUS 2 string model²² are displayed in Fig. 2b. It is successful in predicting the proton rapidity distribution. The main difference in the two models is the inclusion of breakup of leading diquarks in VENUS 2. Relativistic quantum molecular dynamics²³ calculations are also successful in reproducing the measured proton rapidity distributions.

Transverse energy distributions have been measured and studied extensively by the NA34,²⁴ NA35¹¹ and WA80²⁵ Collaborations. In order to relate the measured transverse energy to nuclear stopping, the ratio E_t/E_t^{\max} is formed, where E_t is the transverse energy measured in a given acceptance and E_t^{\max} is the maximum transverse energy possible in 4π solid angle, assuming all the energy is emitted isotropically in the center-of-mass of the participants. The measured E_t in each experimental acceptance is extrapolated to 4π solid angle and compared to the calculated value of E_t^{\max} . The amount of nuclear stopping (in percent) is reflected by the ratio E_t/E_t^{\max} . The amount of stopping for 60 GeV/n oxygen on various targets increases from 0.7 for light targets (Al) to 0.9 for heavy targets (Au). For 200 GeV/n oxygen and sulphur projectiles this range is from 0.4 to 0.7. This is to be compared to "full" stopping measured at 14.5 GeV/n.²⁶ The energy densities calculated using Bjorken kinematics²⁷ range from 1.6 to 3.3 GeV/fm³ for 200 GeV/n oxygen incident on light to heavy targets. These stopping and energy density values are derived from the tails of the E_t distributions. They vary slightly from experiment to experiment and depend strongly upon the level of cross section to which one is sensitive.

Time Evolution of Collision

Transverse Mass and Momentum Distributions

The transverse mass (m_t) distributions of produced particles, mainly pions, have the potential of providing information on the freezeout temperature in the low m_t part of the spectrum ($m_t < m_\pi$), hydrodynamical flow effects at $m_t \sim m_\pi$, and the primordial, critical temperature²⁸ of the system prior to expansion and freezeout at high m_t ($m_t \gg m_\pi$). In the absence of flow effects the

²⁰ S. Wenig, University of Frankfurt, Ph.D. thesis (1990), unpublished.

²¹ H. Stroebele et al., University of Frankfurt Preprint (1990).

²² K. Werner, BNL Preprint BNL-42 435 (1989).

²³ H. Sorge et al., Ann. Phys. 192 (1989) 266.

²⁴ J. Schukraft et al., Nucl. Phys. A498 (1989) 79c.

²⁵ G.R. Young et al., Nucl. Phys. A498 (1989) 53c.

²⁶ see Y. Miake, Proceedings of this Workshop.

²⁷ J.D. Bjorken, Phys. Rev. D27 (1983) 140.

²⁸ L. Van Hove, Phys. Lett. B118 (1982) 138.

lower part of the m_t spectrum should reflect the freezeout conditions. However, hydrodynamical flow would distort the spectrum and these flow effects might be identified in the m_t distributions for various types of particles and colliding systems. Displayed in Fig. 3 are transverse mass distributions, where $m_t = \sqrt{p_t^2 + m^2}$, of various types of particles at midrapidity for central collisions of 200 GeV/n O + Au and S + S. Plotted are $m_t^{-3/2} dn/dm_t$ as a function of m_t . Using relativistic thermodynamics as developed by Hagedorn²⁹ for a single isotropic fireball, a Boltzmann distribution after integration over rapidity gives $dn/dm_t = \text{constant } m_t^{3/2} \exp(-m_t/T)$ for large m_t/T . Thus at large m_t , $m_t^{-3/2} dn/dm_t$ plotted as a function of m_t should be a negative exponential with a single slope and temperature T for all particles. This appears to be the case for the measured Λ , K^0 and proton distributions as well as the large m_t regime of the π^- spectra. The straight lines in Fig. 3 correspond to $dn/dm_t = \text{constant } m_t^{3/2} \exp(-m_t/T)$ with $T = 200$ MeV. Is this the critical transition temperature?

The measured m_t distributions of pions are generally nonthermal in shape and may be a complicated mixture of the effects of freezeout, flow and possibly a critical temperature. Using the velocity of sound in an ultrarelativistic gas, $c/\sqrt{3}$, an estimate can be made of the m_t regime where hydrodynamic flow will have a large effect. Hydrodynamic flow would have its greatest effect in the low m_t part of the m_t spectrum, $m_t < 1.22 m_\pi$. Recent analysis³⁰ of this data and that for π^0 production from WA80³¹ in a radial flow model concludes that the spectra can be fit with an average radial flow velocity of approximately $c/2$ and a freezeout temperature of 100 MeV. The initial temperature in this model before expansion is 200 MeV, similar to that derived from the high m_t part of the particle spectra of Fig. 3.

The general features of the m_t distributions for the produced particles are surprisingly well reproduced by the radial flow model. Although details of the spectra can be reproduced by the model, they may actually have more complicated origins. Displayed in Figs. 4a and b are ratios of O + Au and p + Au data with respect to minimum bias p + p data³² as a function of transverse momentum p_t . An enhancement at low and high p_t , i.e. $p_t < 0.2$ GeV/c and $p_t > 1.0$ GeV/c, is observed in both systems. The p_t distribution for p + Au in central collisions exhibits effects which must have similar origin and interpretations as in the O + Au data. These effects in the ratios plotted in Figs. 4a and b have also been observed in very high charged-particle multiplicity (N_{ch}) p + p and $\alpha + \alpha$ events at $\sqrt{s_{nn}} = 63$ and 31.2 GeV, respectively.³³ These ratios relative to minimum bias data are plotted in Figs. 5a and b for intermediate ($6 \leq N_{ch} \leq 10$) and high ($18 \leq N_{ch}$) multiplicity events. The enhancements at low and high p_t are not observed in the low and intermediate multiplicity data. The structure of the ratios for high N_{ch} events is remarkably similar to those of the central p + Au and O + Au data in Figs. 4a and b. The marked similarity of central p + Au and O + Au collisions to very high multiplicity "hard-scattering" p + p and $\alpha + \alpha$ collisions suggests an explanation is necessary at the quark-parton level. Similar

²⁹ R. Hagedorn, CERN 71-12 (1971); GSI-Report 81-6 (1981) 236; Proceedings of Quark Matter 84, ed. K. Kajantie, Springer-Verlag (1985) 53.

³⁰ K.S. Lee and U. Heinz, Z. Phys. C43 (1989) 425.

³¹ R. Santo et al., Nucl. Phys. A498 (1989) 391c; L. Dragon, Ph.D. thesis, University of Muenster (1989).

³² NA5 Collaboration, private communication.

³³ W. Bell et al., Phys. Lett. B112 (1982) 271; A. Karabarbounis et al., Phys. Lett. B104 (1981) 75; A.L.S. Angelis et al., Phys. Lett. B116 (1982) 379.

p_t distributions have been measured in specialized spectrometer experiments: for 200 GeV/n heavy ions in the NA34 experiment at CERN³⁴ and for $\sqrt{s} = 1.8$ TeV pp at FermiLab.³⁵

Hanbury Brown and Twiss (HBT) correlations

Hanbury Brown and Twiss (HBT) correlations³⁶ between negative pions have been measured for various systems by the NA35 Collaboration. The approach involves a Gaussian parameterization³⁷ of the pion-emitting source, at the time when interactions cease (freezeout), using a transverse radius R_T , a longitudinal radius R_L and a chaoticity parameter Λ . Another parameterization³⁸ of the source distribution which is Lorentz-covariant and incorporates an inside-outside cascade for the collision dynamics utilizes the parameters R_T , Λ and the source lifetime τ_0 . A value of $\Lambda = 1$ corresponds to incoherent emission from the source. Values of $\Lambda < 1$ correspond to increasing coherence, with $\Lambda = 0$ total coherence. Displayed in Figs. 6a-c are the HBT correlations for negative pions over the measured rapidity range ($1 < y < 4$), away from midrapidity ($1 < y < 2$) and at midrapidity ($2 < y < 3$), respectively, in central collisions of 200 GeV/n O + Au.³⁹ Also shown for comparison in Fig. 6d is the expected absence of a correlation in the Lund/FRITIOF model calculation. The pions at $2 < y < 3$, midrapidity in the effective $^{16}\text{O} + \text{Au}$ center-of-mass ($y_{\text{cm}} = 2.5$), are found to originate from a large ($R_T = 8.1 \pm 1.6$ fm), relatively chaotic ($\Lambda = 0.7 \pm 0.2$), long-lived ($\tau_0 = 6.4 \pm 1.0$ fm/c) source. Away from midrapidity the pions reflect a source of the size of the incident projectile ($R_T = 4.3 \pm 0.6$ fm), less chaotic ($\Lambda = 0.34 \pm 0.07$), and fairly short-lived ($\tau_0 = 2.5 \pm 1.0$ fm/c).

This picture suggests the formation of a thermalized fireball at midrapidity. Considering the large number of produced particles, mostly pions, near midrapidity in central collisions of O + Au at 200 GeV/n (approximately 120 - 140 per unit rapidity^{12,39}) and the $\pi\pi$ strong interaction cross sections, one predicts a similar size ($R \sim 8$ fm) for a thermalized system of pions at freezeout. Preliminary NA35 results on HBT correlations for negatively-charged pions from central 200 GeV/n S + Ag and S + Au collisions⁴⁰ exhibit these same effects, a large source of midrapidity pions and a small source for those detected away from midrapidity. Examining the S + Ag and S + Au data as a function of the pion multiplicity, the source radius for pions at midrapidity is observed to increase with the multiplicity. This is also observed globally in pp, hadron-hadron and nucleus-nucleus data for R_T as a function of rapidity density. A compilation⁴¹ of these results is presented in Fig. 7. The R_T increases approximately as $R_T \sim (dn/dy)^{1/2}$. For the lighter S + S system at midrapidity R_T is found to be near that of the incident projectile, R_L is smaller than R_T , and Λ is low similar to those observed in HBT measurements in e^+e^- and hadron-hadron collisions.

³⁴ B. Jacak et al., to be published in the Proceedings of the Eighth International Conference on Ultra-Relativistic Nucleus-Nucleus Collisions, Menton, France, May 1990.

³⁵ T. Alexopoulos et al., Phys. Rev. Lett. 64 (1990) 991.

³⁶ R. Hanbury Brown and R.Q. Twiss, Nature 177 (1956) 27 and Nature 178 (1956) 1046.

³⁷ F.B. Yano and S.E. Koonin, Phys. Lett. B78 (1978) 556.

³⁸ K. Kolehmainen and M. Gyulassy, Phys. Lett. B180 (1986) 203.

³⁹ A. Bamberger et al., Phys. Lett. B203 (1988) 320.

⁴⁰ P. Seyboth, Proceedings of the Workshop on Heavy Ion Physics at the AGS, Brookhaven National Laboratory Report BNL-44911, p.261.

⁴¹ R. Stock, University of Frankfurt preprint IKF90-3 (1990), to be published in Annalen der Physik.

The effects on the HBT correlations of the decays of hadronic resonances,⁴² hydrodynamical expansion, and space-time correlations of the source must be considered in interpretations of the results. The emerging picture from HBT correlations suggests that detailed measurements of source parameters as a function of the various orientations of the relative momentum of the particle-pair may provide information on the time evolution of the collision and possibly the existence of a QGP.⁴³

III. Quark-Gluon Plasma Signatures

Suppression of J/ψ Production in QGP

In analogy to the Debye screening of electrons in electrodynamics and plasma physics, Debye screening of the quark color charge would result in deconfinement into a quark-gluon plasma. Furthermore, the color screening is predicted² to prevent $c\bar{c}$ binding into a J/ψ in the deconfinement region. In hadron-hadron collisions $c\bar{c}$ pairs can be produced in either $g\bar{g}$ or $q\bar{q}$ interactions. However, in nucleus-nucleus collisions the $c\bar{c}$ will appear in a deconfining environment at high temperature and high density. If the Debye radius is less than the radius of the J/ψ at temperature T , then formation of the J/ψ is prohibited assuming the plasma lifetime is longer than the formation time of the J/ψ from $c\bar{c}$. Therefore, observation of J/ψ suppression in nucleus-nucleus interactions might signify formation of the plasma. This is a possible QGP signature since the J/ψ yield would not be reduced in passage through the nuclear matter due to its small nuclear absorption.⁴⁴

The NA38 Collaboration at CERN has measured the J/ψ yield⁴⁵ in various nucleus-nucleus systems at 200 GeV/n. The experiment consists of a muon-pair spectrometer to measure the invariant mass spectrum of like-sign and opposite-sign muon pairs along with associated calorimetry for global event characterization. The invariant mass spectra for opposite-sign muon pairs and the background, consisting of a combination $2\sqrt{N^{++}N^{--}}$ of the two possible like-sign pair spectra, N^{++} and N^{--} , are displayed in Fig. 8. Subtraction of these two spectra yields the prompt dimuon spectrum of Fig. 8. The J/ψ resonance can be seen prominently above a steeply-falling continuum composed primarily of Drell-Yan pairs, low-mass resonance decays and charmed-particle decays. Displayed in Fig. 9 is the ratio (S) of the J/ψ yield to that of the continuum for several systems as a function of the transverse energy (E_t) measured in the experiment. Larger values of E_t are associated with smaller impact parameter collisions as described in the section on collision geometry above. Therefore, the ratio of the J/ψ yield to that of the continuum is suppressed for higher E_t , i.e. more central collisions.

If the measured suppression of the J/ψ yield is, in fact, due to color screening of $c\bar{c}$ pairs in a QGP, then the suppression is predicted to be stronger at lower p_t values of the J/ψ .⁴⁶ This has been observed by NA38 as shown in Fig. 10. The ratio $R(p_t) = S(p_t)^{\text{high } E_t} / S(p_t)^{\text{low } E_t}$ is

⁴² M. Gyulassy and S. Padula, Phys. Lett. B217 (1988) 181.

⁴³ M. Gyulassy, Phys. Rev. Lett. 48 (1982) 454; S. Pratt, Phys. Rev. D33 (1986) 1314; G.F. Bertsch, Nucl. Phys. A498 (1989) 173c.

⁴⁴ R. Anderson et al., Phys. Rev. Lett. 38 (1977) 263; J. Branson et al., Phys. Rev.Lett. 38 (1977) 1334.

⁴⁵ J.Y.Grossiord et al., Nucl. Phys. A498 (1989) 249c.

⁴⁶ F. Karsch and R. Petronzio, Phys. Lett. B193 (1987) 105.

J.P. Blaizot and J.Y. Ollitrault, Phys. Lett. B199 (1988) 499 and Z. Phys. C38 (1988) 627.

M.C. Chu and T. Matsui, Phys. Rev. D37 (1988) 1851.

presented in Fig. 10, where $S(p_t)$ is the J/ψ to continuum ratio as a function of p_t for high and low E_t events, respectively. The measured p_t -dependence of J/ψ suppression can be described in terms of quasielastic initial-state parton scattering and final-state inelastic scattering in a dense hadron gas,⁴⁷ also shown in Fig. 10. The quasielastic initial-state scattering of partons from the projectile and target prior to the hard $c\bar{c}$ or Drell-Yan production causes a p_t variation in the J/ψ yield which is also observed in hadron-nucleus measurements. This effect is also incorporated in a description of J/ψ production⁴⁷ for hadron-nucleus and nucleus-nucleus reactions. The final-state inelastic processes in a dense hadron gas reduce the J/ψ yield at high p_t as seen in Fig. 10. To be able to describe the J/ψ suppression data in Fig. 10 sufficient final-state inelastic scattering of the J/ψ is necessary. This is accomplished in the model by incorporating energy and particle densities of the hadron gas similar to those expected for the QGP or mixed hadron gas - QGP phase.⁴⁸ Systematic studies of the p_t dependence of the continuum, as well as J/ψ and Drell-Yan production in various hadron-nucleus systems are necessary to further constrain the initial-state scattering in these models and to distinguish between possible QGP-induced suppression and suppression due to collision effects.

Enhancement of Strangeness Production

One of the earliest predictions for a signature of the deconfinement transition is an enhancement of s and \bar{s} quarks in a quark-gluon plasma in thermal and chemical equilibrium.³ The strangeness enhancement is a result of the Pauli principle suppression of uu and dd pair production in favor of $s\bar{s}$ pairs in the initial u and d -rich environment remaining from the incident nuclei.⁴⁹ Furthermore, the \bar{u} and \bar{d} quarks annihilate with u and d quarks, while the $s\bar{s}$ annihilation occurs less frequently until saturation of the s and \bar{s} abundances. Most calculations predict an enhancement in the observed \bar{s} yield as a signature of plasma formation while s quark yields, although enhanced, differ only slightly in a plasma compared to a hadron gas. The actual observation of s enhancement after plasma formation is severely complicated by the spacetime evolution of the collision process, making it difficult to discriminate between the hadronization products of a quark-gluon plasma and those of a chemically-equilibrated hadron gas. However, it is highly unlikely that hadronic processes in the nonplasma phase are best represented by an equilibrium hadron gas. Thus, the dynamics complicate the issue and must be understood.

Dynamical approaches predict^{50,51} a separation of strangeness during the hadronization process in a non-zero baryo-chemical potential environment. Most of the strangeness content of the reaction is carried away by kaons, since they are the lightest strange particles and therefore energetically the easiest to produce. During the mixed phase, consisting of plasma and hadron gas, s quarks hadronize mainly into K^+ and K^0 mesons while the \bar{s} quarks become concentrated in the plasma regions. The hadronization of hyperons, K^- and \bar{K}^0 mesons from s quarks occurs much later. An s -enriched plasma results and a byproduct, the production of strange droplets of matter⁵², could provide information on the existence of a QGP. Therefore, the K^+ mesons

⁴⁷ S. Gavin and M. Gyulassy, Phys. Lett. B214 (1988) 241.

⁴⁸ S. Gavin, M. Gyulassy and A. Jackson, Phys. Lett. B208 (1988) 257.

⁴⁹ Other important factors which contribute to the enhanced strangeness are: the large numbers of gluons, the lower strangeness mass threshold and the higher \bar{s} to \bar{q} ratios in the QGP.

⁵⁰ U. Heinz, K.S. Lee and M.J. Rhoades-Brown, Mod. Phys. Lett. A2 (1987) 153.

⁵¹ C. Geiner, P. Koch and H. Stoecker, Phys. Rev. Lett. 58 (1987) 1825.

⁵² E. Whitten, Phys. Rev. D30 (1984) 272.

should provide information on the early stages of the collisions. The slopes of the K^+ and K^- spectra are expected to reflect their hadronization temperatures.⁵³ In the absence of a QGP, the K^+ slopes will reflect a higher temperature than the K^- 's which hadronize later. If a QGP were formed, then the K^+ slopes will reflect lower temperatures than in the purely hadronic case due to energy bound in the latent heat of the QGP transition. Furthermore, if a QGP were formed, the K^- slopes and those of other hadrons will reflect higher temperatures than in the non-QGP scenario due to the additional entropy per baryon produced in the QGP. Thus, the K^+ and K^- spectra will be products of a complicated mixture of various dynamical processes.

The NA34 Collaboration has measured K/π ratios and kaon spectra⁵⁴ in a magnetic spectrometer. Displayed in Fig. 11 are the K^+/π^+ and K^-/π^- ratios as a function of p_t for S + W and p + W at 200 GeV/n incident energy near $y = 1$. Also plotted are these ratios for p + p reactions. The K^-/π^- ratios for S + W and p + W are consistent with those measured in p + p reactions. The K^+/π^+ ratios for S + W increase as a function of p_t from values consistent with p + W and p + p reactions at low p_t to values 2 to 3 times higher than those at high p_t . The K^+/π^+ ratios for p + W are slightly higher than those measured in p + p reactions. No significant change in these ratios as a function of centrality is observed in the S + W collision.⁵⁴ These results are consistent with measurements at lower energies by the E802 group at the AGS⁵⁵ and have not been explained in terms of normal hadronic interactions.

The slopes of the proton, K^+ and π^- distributions of invariant cross section as a function of transverse mass m_t have been measured by the NA34 Collaboration for the S + W system near $y = 1$.⁵⁴ They are in agreement with those reported for proton, Λ , K^0_s and π^- by the NA35 Collaboration and presented above for S + S and O + Au at $y = y_{cm} = 3$. These slope values are approximately 200 MeV. The K^- spectra for S + W exhibit a significantly lower slope of 107 ± 26 MeV. The observation of larger values of slope parameters for the K^+ than the K^- is consistent with an interpretation in terms of normal hadronic interactions with possible collective flow during expansion as described above.

The NA35 Collaboration has measured the production of strange particles in 60 and 200 GeV/n p + Au and O + Au⁵⁶ and in 200 GeV/n S + S collisions⁵⁷ using a streamer chamber. Displayed in Fig. 12 is the mean number of Λ particles per event as a function of the mean charged particle multiplicity of the events for S + S reactions. The Λ production increases with centrality of the collision at a rate faster than that predicted by the Lund/FRITIOF model and faster than a superposition model of nucleon-nucleon data. The same dependence is also observed for Λ and K^0 production. For central collisions the Λ yield is more than a factor of two larger than predicted by any of the models, including a hadron gas model, with the exception of a parton gas model. For details of the models and comparisons see Refs. 57. The ratios of $\langle n(\Lambda) \rangle / \langle n(\pi^-) \rangle$, $\langle n(\bar{\Lambda}) \rangle / \langle n(\pi^-) \rangle$ and $\langle n(K^0) \rangle / \langle n(\pi^-) \rangle$ also increase with centrality of the collision and are approximately a factor of 2 higher for S + S than for p + S over the same acceptance.⁴⁰ These enhanced strange particle production yields have yet to be explained in terms of simple nuclear phenomena.

⁵³ U. Heinz, K.S. Lee and M.J. Rhoades-Brown, Phys. Rev. Lett. 58 (1987) 2292.

⁵⁴ H. van Hecke et al., to be published in the Proceedings of the Eighth International Conference on Ultra-Relativistic Nucleus-Nucleus Collisions, Menton, France, May 1990.

⁵⁵ Y. Miake, Proceedings of this Workshop.

⁵⁶ A. Bamberger et al., Z. Phys. C43 (1989) 25.

⁵⁷ J. Bartke et al., U. Frankfurt Preprint (1990); M. Gazdzicki et al., Nucl. Phys. A498 (1989) 375c.

The WA85 Collaboration has preliminary results^{58,59,60} on strange and multi-strange baryon production in the reactions 200 GeV/n S + W and p + W using the large acceptance Ω magnetic spectrometer at CERN. The yields of multiply-strange baryons are expected to be very sensitive to the existence of a QGP because they contain more than one strange quark.⁶¹ The ratios of the mean numbers of $\bar{\Xi}^-$ and Ξ^- measured in the acceptance $p_t > 1$ GeV/c and $2.3 < y < 3.0$ are $\langle \bar{\Xi}^- \rangle / \langle \Xi^- \rangle = 0.43 \pm 0.07$ for S + W and $\langle \bar{\Xi}^- \rangle / \langle \Xi^- \rangle = 0.27 \pm 0.06$ for p + W.⁶⁰ These ratios are unexpectedly large; their significance and the observed increase from p + W to S + W are of extreme interest and under intensive theoretical investigation.⁶² The $\langle \Lambda \rangle / \langle \Lambda \rangle$ ratio for the same acceptance is 0.24 ± 0.08 , which is consistent with a measurement of 0.29 ± 0.10 from the NA35 Collaboration for the same acceptance. These values are similar to those measured at midrapidity in p + p and p + A interactions. The WA85 Collaboration finds an increase and then leveling off in the yield of Λ 's and in the ratio of the numbers of Λ 's to negative particles as a function of rapidity density at midrapidity. This observation is similar to that displayed in Fig. 12, but for a different system. A comparison of strangeness production in nucleus-nucleus versus proton-nucleus interactions can be made by studying the yield of Λ 's normalized to the yield of negative hadrons (h^-). WA85 finds $(\langle \Lambda \rangle / \langle h^- \rangle)_{S+W} = 1.7 (\langle \Lambda \rangle / \langle h^- \rangle)_{p+W}$, i.e. the yield of Λ 's relative to negative hadrons increases a factor of 1.7 in going from p + W to S + W. This is comparable to the value $(\langle \Lambda \rangle / \langle h^- \rangle)_{S+S} = 1.77 (\langle \Lambda \rangle / \langle h^- \rangle)_{p+S}$ from NA35.^{40,57}

The NA38 Collaboration has extended its muon pair measurements, described above for J/ψ production, to the lower pair-mass region of the ρ , ω and ϕ resonances. An enhancement in the ϕ production rate is expected from a QGP.⁶³ In order to reduce the background, cuts were imposed to accept only muon pairs with $p_t > 1.3$ GeV/c and $2.8 < y < 4$. Displayed in Fig. 13 are the resultant invariant mass distributions for 200 GeV/n p + U, O + U and S + U.⁶⁴ Peaks are seen in the mass region of the J/ψ and in the vector meson mass region. Fits were made assuming contributions to the spectrum from the $(\rho + \omega)$, ϕ and the continuum. The ratio $n(\phi)/n(\rho + \omega)$ increases as the mass of the colliding system increases, reaching a value $n(\phi)/n(\rho + \omega) = 0.59 \pm 0.02$ for the S + U system. The ϕ production was also studied as a function of centrality.⁶⁵ Displayed in Fig. 14 are the ratios of $n(\phi)/n(\rho + \omega)$ in O + U or S + U collisions to $n(\phi)/n(\rho + \omega)$ in p + U collisions as a function of $E_t/A^{2/3}$. The quantity $E_t/A^{2/3}$ is proportional to the energy density in the initial stages of the collision according to the Bjorken formula.²⁷ Therefore, the ϕ production rate increases with the centrality of O + U and S + U collisions up to a factor of 3 times the rate measured for p + U. This is very similar to the approximately twofold increase in the strange particle yields for Λ , $\bar{\Lambda}$ and K^0 for central collisions versus peripheral collisions of S

⁵⁸ N.J. Narjoux et al., to be published in the Proceedings of the Eighth International Conference on Ultra-Relativistic Nucleus-Nucleus Collisions, Menton, France, May 1990.

⁵⁹ D. Evans et al., to be published in the Proceedings of the Eighth International Conference on Ultra-Relativistic Nucleus-Nucleus Collisions, Menton, France, May 1990.

⁶⁰ S. Abatzis et al., to be published in the Proceedings of the International Workshop on Quark-Gluon Plasma Signatures, 1 - 4 October, 1990, Strasbourg, France.

⁶¹ M. Jacob and J. Rafelski, Phys. Lett. B190 (1987) 173.

⁶² for example see H.C. Eggers and J. Rafelski, University of Arizona preprint AZPH-TH/90-28 (1990).

⁶³ A. Shor, Phys. Rev. Lett. 54 (1985) 1122.

⁶⁴ M.C. Abreu et al., presented at the XXVth Recontres de Moriond, Les Arcs, France, March 11 - 17, 1990.

⁶⁵ A. Baldisseri et al., Annecy preprint LAPP-EXP-89-15, to be published in the Proc. of the Intern. Europhys. Conf. on High Energy Physics, Madrid (1989).

+ S measured by NA35. Since the ρ -nucleon and ω -nucleon cross sections have been estimated to be approximately 3 times larger than the ϕ -nucleon cross section,⁶⁶ rescattering effects and absorption in the nuclear medium are expected to increase the $n(\phi)/n(\rho + \omega)$ ratio. Inclusion of rescattering effects into a model which assumes a dense collision region,⁶⁷ as required to fit the J/ψ data, quantitatively describes the ϕ production data.

Information on Other Signatures

The possible observation of a *critical transition temperature* in the p_t and m_t spectra of produced particles was discussed above. An in-depth presentation of measurements of *fluctuations and intermittency* in relativistic heavy ion collisions as possible QGP signatures appears elsewhere in this Workshop.⁶⁸ No statistically significant signal in the inclusive photon to π^0 ratio has been observed beyond that expected from hadronic decays.⁶⁹ Thus, *direct photons* from a QGP have yet to be seen.

IV. Summary and Conclusions

Geometry plays an important role in the dynamics of relativistic heavy ion collisions. Information from experiments support a "clean-cut" geometrical picture. In central collisions a large amount of energy is transformed from the relative motion of the incident nuclei into produced particles and transverse degrees of freedom. There is a considerable amount of nuclear stopping: large numbers of baryons are observed near midrapidity and the transverse energy distributions extend to values of energy densities near that of a QGP phase transition. The high end of the m_t spectra for various types of particles suggests a common, single-temperature source near $T = 200$ MeV. Hanbury Brown Twiss correlations between pions depict a large, incoherent source of pions at midrapidity and a small, more coherent source away from midrapidity. The predicted suppression of J/ψ production for a QGP is observed, but has been explained in terms of initial-state parton scattering and final-state inelastic scattering in a dense hadronic gas. An enhancement in the production of strange particles (Λ , $\bar{\Lambda}$, K^0 , K^+ , $\bar{\Xi}^-$ relative to Ξ^- , ϕ relative to $\rho + \omega$) similar to that predicted for a QGP has been measured. This enhancement increases with centrality of the collision. The enhanced production of the ϕ relative to $\rho + \omega$ has been described in terms of rescattering effects in a dense hadronic medium. The production rates for the other strange particles that have been measured have yet to be described in terms of normal hadronic physics. Although unambiguous evidence for a QGP has not been found, it appears that the necessary preconditions determined from the dynamical observables are right: the energy densities extracted from data are of the order of a few GeV/fm^3 , the particle densities a few fm^{-3} and the collision volume a few times 10 fm^3 . Furthermore, the models which presently describe quantitatively the observed enhanced J/ψ and strangeness production require particle densities similar to those required for QGP formation. Systematic data for the heaviest systems and detailed theoretical calculations encompassing the many observables that have been measured are necessary before any definitive statement can be made as to the presence of a QGP in these interactions.

⁶⁶ R. Spital and D.R. Yennie, Phys. Rev. D9 (1974) 138.

⁶⁷ P. Koch, U. Heinz and J. Pisut, Phys. Lett. B243 (1990) 149.

⁶⁸ I. Otterlund, Proceedings of this Workshop.

⁶⁹ F. Plasil et al., Proceedings of the Workshop on Nuclear Dynamics VII, Jackson Hole Wyoming, ed. J. Randrup, Lawrence Berkeley Laboratory Report LBL-28709 (1990).

Acknowledgements

I wish to thank my colleagues in NA34, NA35, NA38, WA80, and WA85 for making available their data prior to publication. This work was supported by the Director, Office of Energy Research, Division of Nuclear Physics of the Office of High Energy and Nuclear Physics of the U.S. Department of Energy under contract DE-AC03-76SF00098.

Figure Captions

Fig.1. The proton rapidity distributions for peripheral (boxes) and central collisions (circles) of 200 GeV/n S + S. The filled symbols correspond to measured points and the open symbols are those points reflected about midrapidity ($y_{cm} = 3$).

Fig.2. The data of Fig.1 compared to the predictions of the string models a) Lund/FRITIOF and VENUS 2.

Fig.3. Transverse mass distributions for various particles in central collisions of 200 GeV/n a) O + Au and b) S + S. The rapidity intervals for a) are on the figure while those for b) are $0.8 < y < 2.0$, $1.5 < y < 3.0$, $1.4 < y < 2.7$ and $1.5 < y < 3.5$ for Λ , p, K^0 and π^- , respectively. The straight lines correspond to a temperature of 200 MeV in the Hagedorn fireball model.

Fig.4. Ratios $R(p_t)$ of the transverse momentum distributions of central a) $^{16}\text{O} + \text{Au}$ and b) p + Au collisions relative to minimum bias p + p collisions at 200 GeV/n. The dashed lines indicate $R(p_t) = 1$. The trigger conditions were a) forward energy trigger FET(56) and b) transverse energy trigger TET(260) with trigger cross sections of 56 and 260 mb, respectively.

Fig.5. Ratios $R(p_t)$ of the transverse momentum distributions of selected charge multiplicity (N_{ch}) in p + p and $\alpha + \alpha$ events at $\sqrt{s_{nn}} = 63$ and 31.2 GeV, respectively, relative to minimum bias data for a) intermediate ($6 \leq N_{ch} \leq 10$) and b) high ($18 \leq N_{ch}$) multiplicity events.

Fig.6. Measured HBT correlation function for negative pions from central collisions of 200 GeV/n O + Au projected onto the relative transverse momentum Q_T axis (for pairs with relative longitudinal momentum $Q_L < 100$ MeV/c) for the rapidity intervals shown (a-c) and for the Lund/FRITIOF model (d).

Fig.7. Compilation of transverse source radii for particle production at midrapidity in hadron-hadron and relativistic heavy ion collisions as a function of the charged-particle rapidity density at midrapidity. See text for details

Fig.8. Invariant mass spectra for opposite-sign muon pairs (OS) and the background, consisting of a combination $2\sqrt{N^{++}N^{--}}$ of the two possible like-sign pair spectra, N^{++} and N^{--} . Subtraction of these two spectra yields the prompt dimuon spectrum shown as data points.

Fig.9. The ratio (S) of the J/ψ yield to that of the continuum for several systems as a function of the transverse energy (E_t). Larger values of E_t are associated with smaller impact parameter collisions.

Fig.10. The ratio $R(p_t) = S(p_t)^{\text{high } E_t} / S(p_t)^{\text{low } E_t}$, where $S(p_t)$ is the J/ψ to continuum ratio as a function of p_t for high and low E_t events, respectively. Model calculations are shown for the p_t -dependence of J/ψ suppression in terms of quasielastic initial-state parton scattering and final-state inelastic scattering in a dense hadron gas. See text for details.

Fig.11. K^+/π^+ (dots) and K^-/π^- (circles) ratios in percent as a function of p_t for a) S + W and b) p + W at 200 GeV/n incident energy. The data cover the rapidity range $0.8 < y < 1.3$. The inner error bars are statistical and the outer are statistical plus systematic. The curves represent the K^+/π^+ (dotted curve) and K^-/π^- (dashed curve) ratios measured for p + p reactions.

Fig.12. The mean number of Λ particles per event as a function of the mean charged particle multiplicity (centrality) of the events for S + S reactions. Also shown are predictions of the

Lund/FRITIOF model, a superposition of nucleon-nucleon data, a hadron gas model and a parton gas model.

Fig.13. Invariant mass distributions for 200 GeV/n p + U, O + U and S + U. Peaks are seen in the mass region of the J/ψ and in the vector meson mass region. The solid curve is the final fit result assuming contributions to the spectrum from the $(\rho + \omega)$, ϕ and the continuum which are represented as dashed, dot-dashed and dotted curves respectively.

Fig.14. For 200 GeV/n p + U, O + U and S + U collisions the ratios of $n(\phi)/n(\rho + \omega)$ to $n(\phi)/n(\rho + \omega)$ in p + U collisions as a function of $E_T/A^{2/3}$.

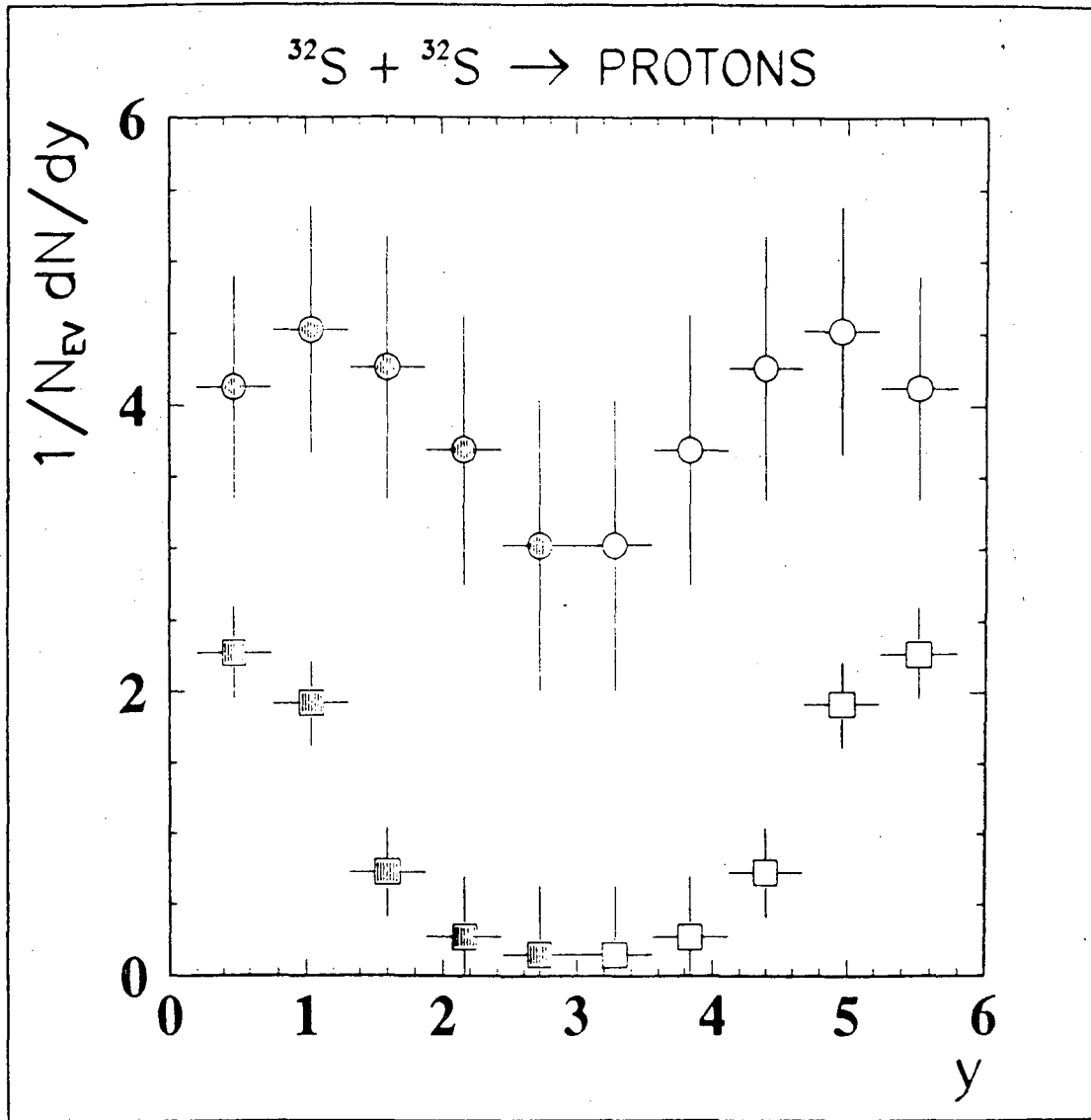


Fig.1

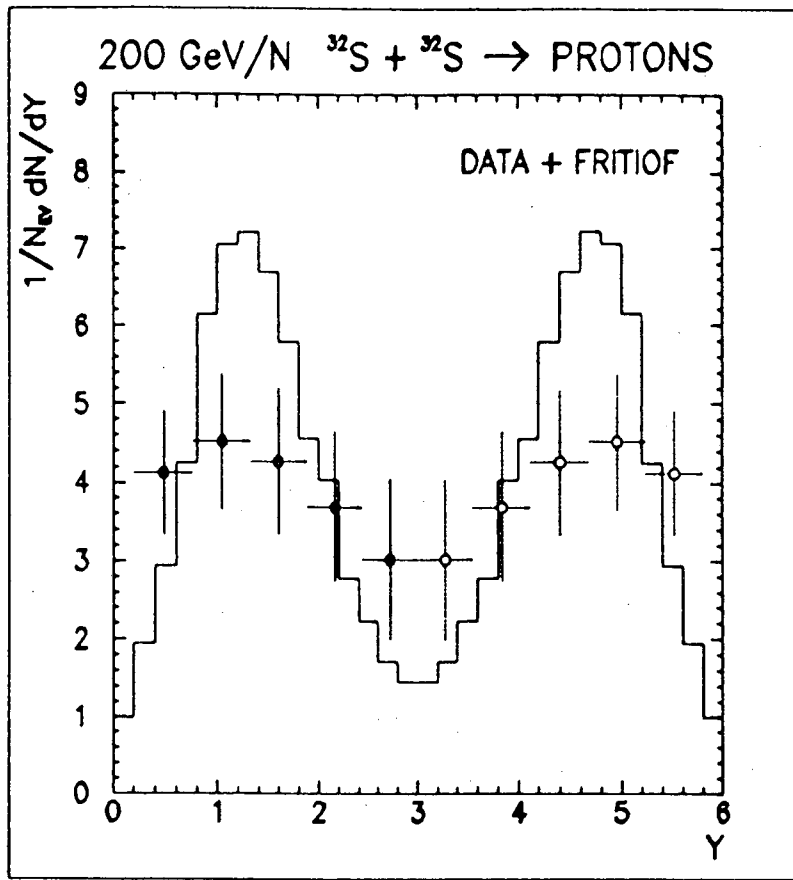
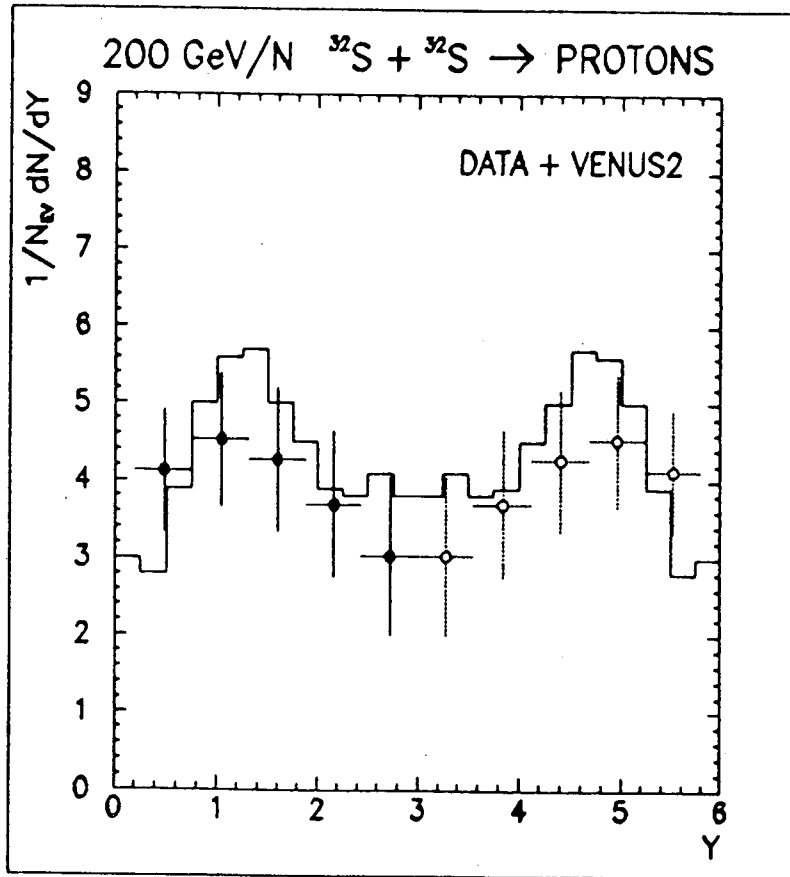


Fig.2



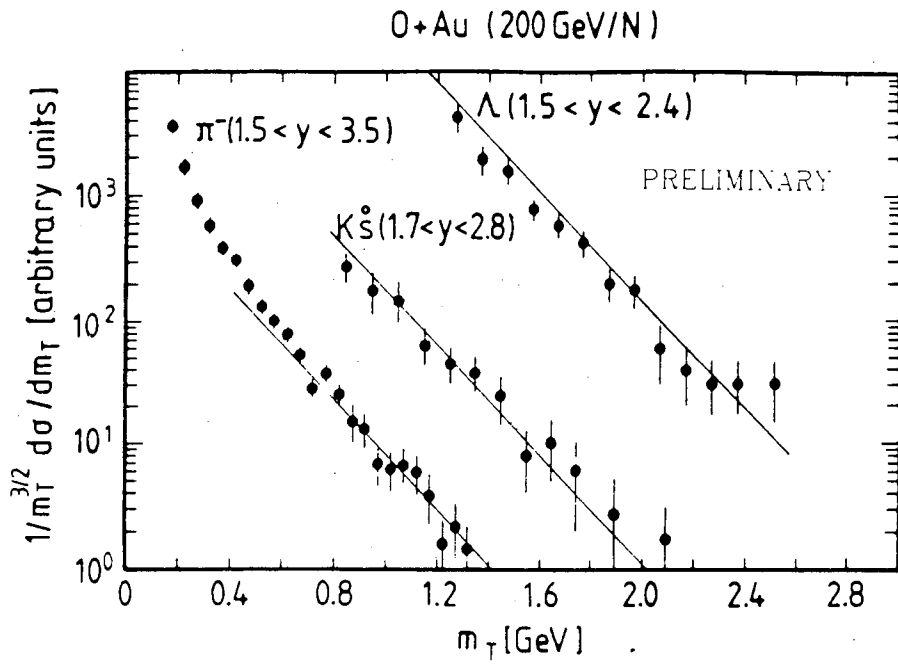
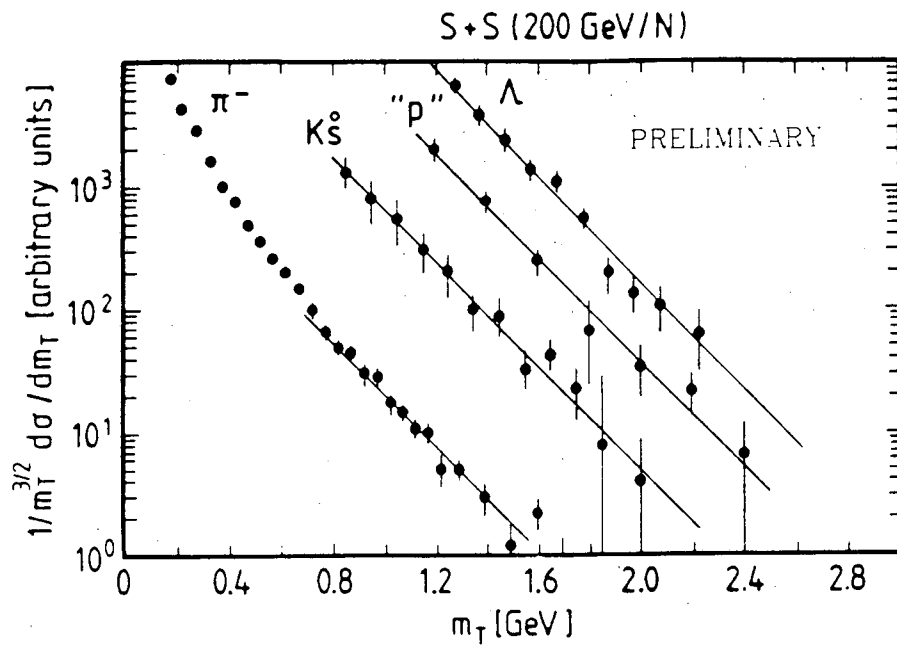


Fig.3



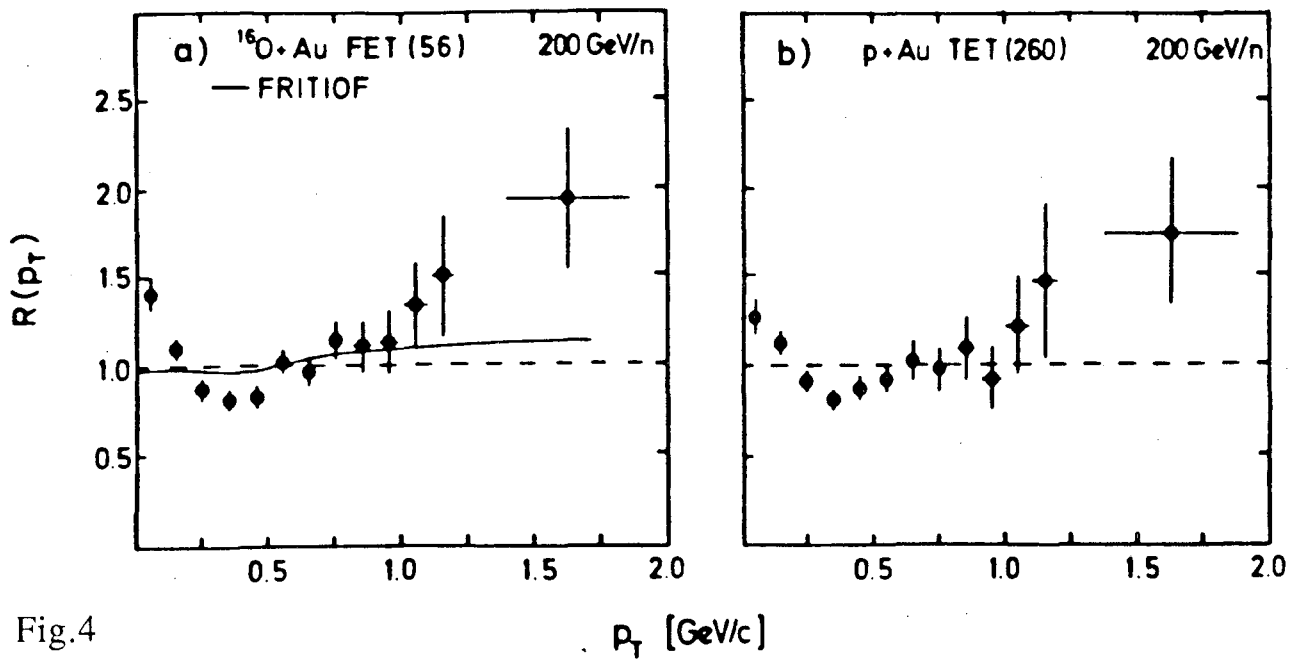


Fig.4

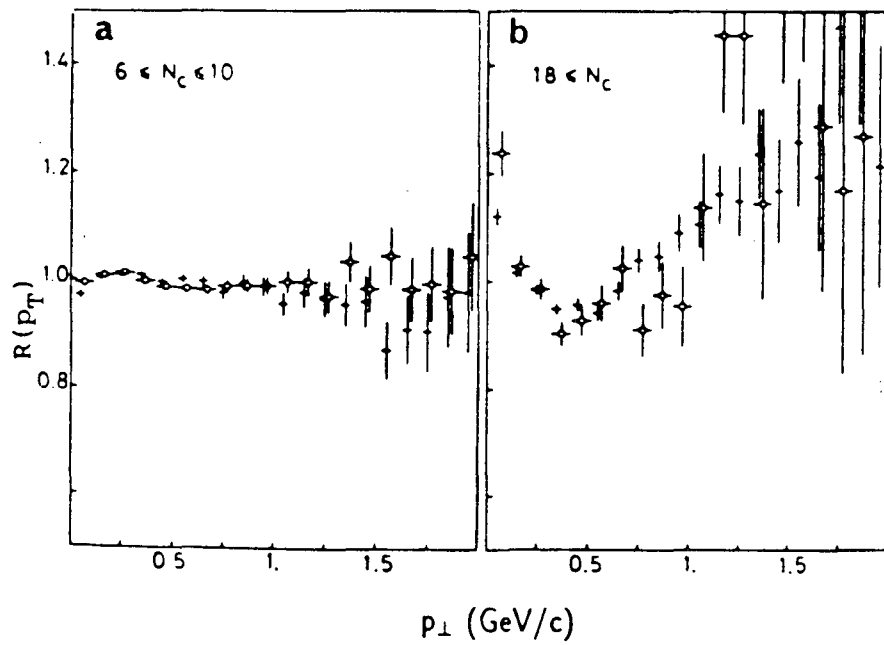


Fig.5

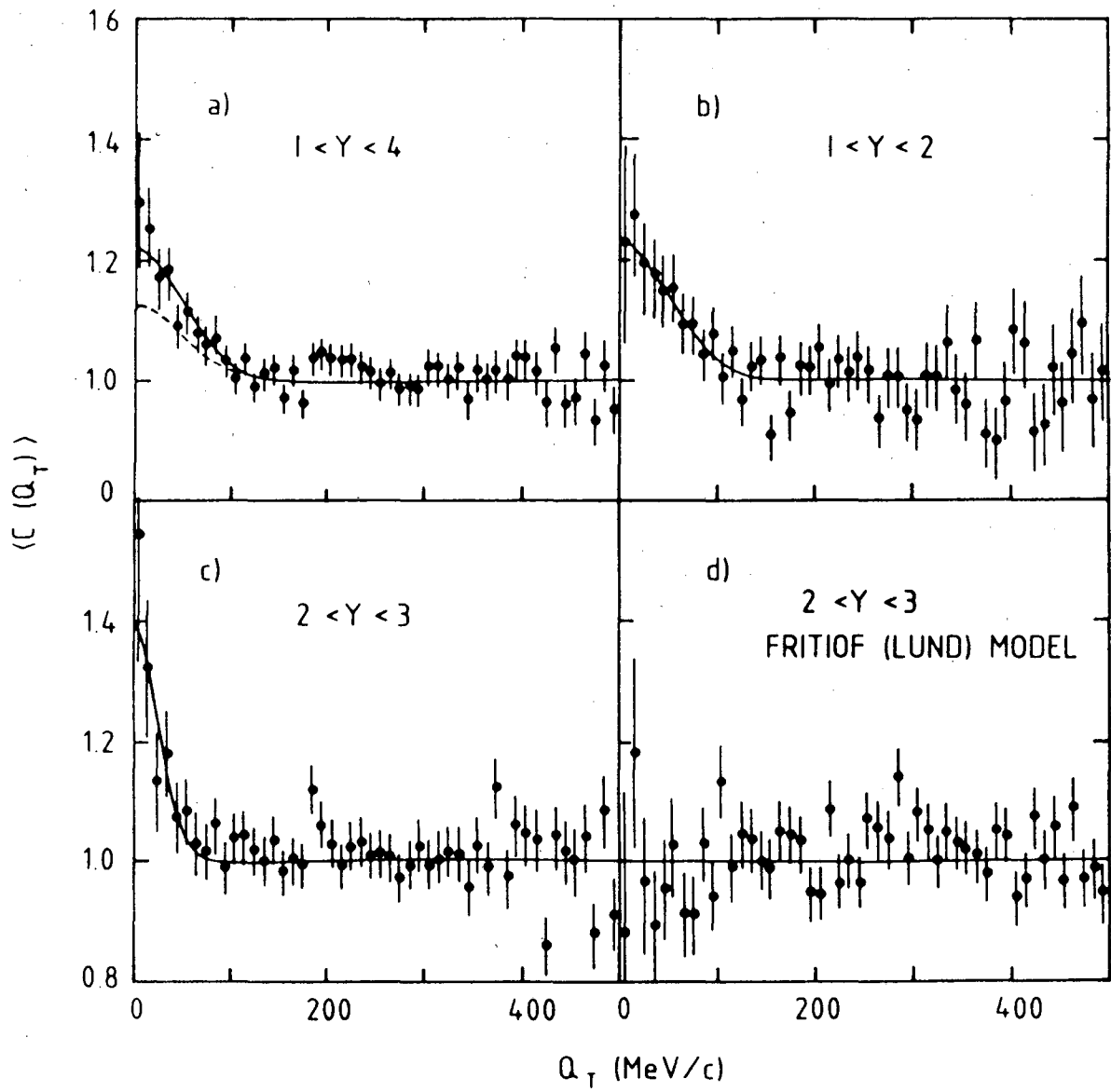


Fig.6

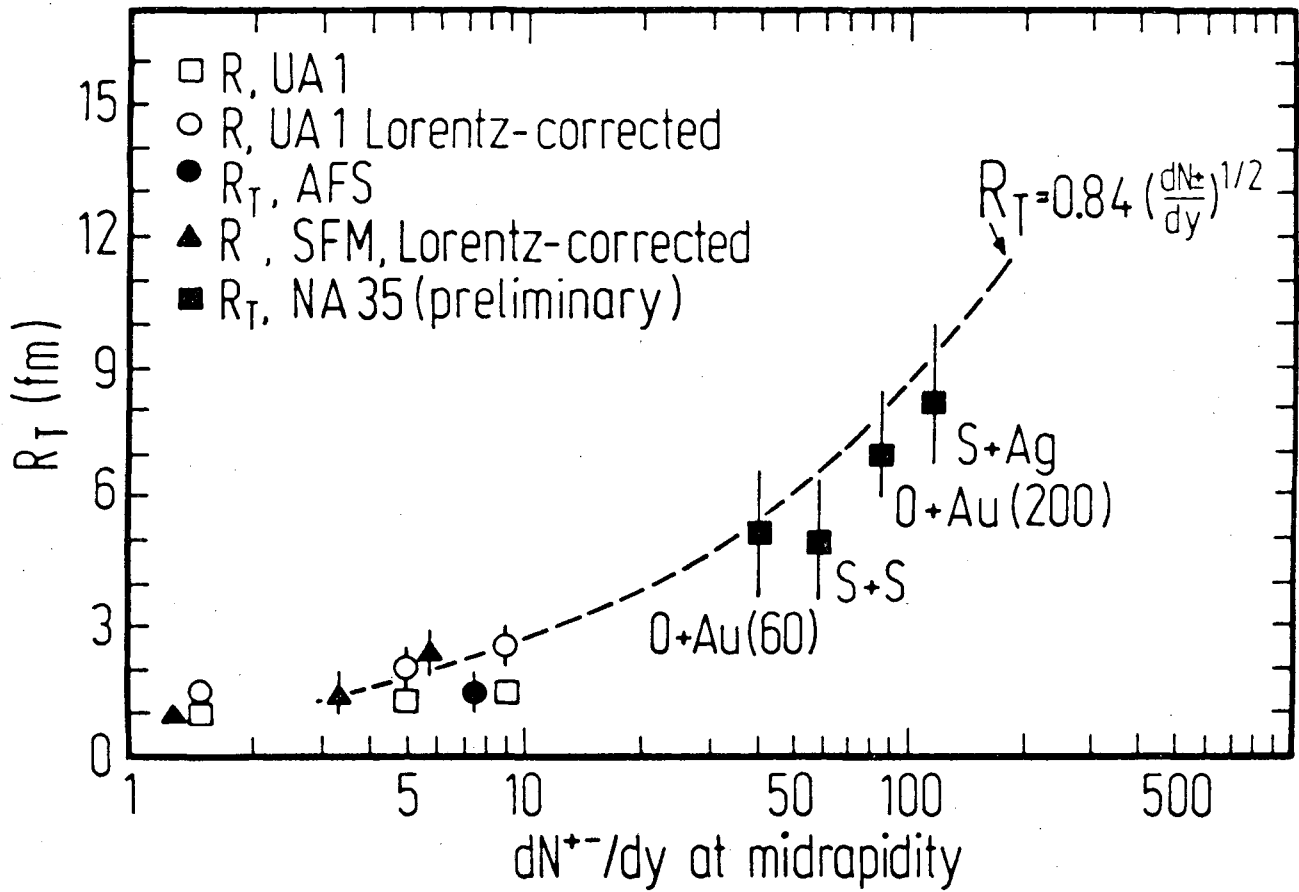


Fig.7

Fig.8

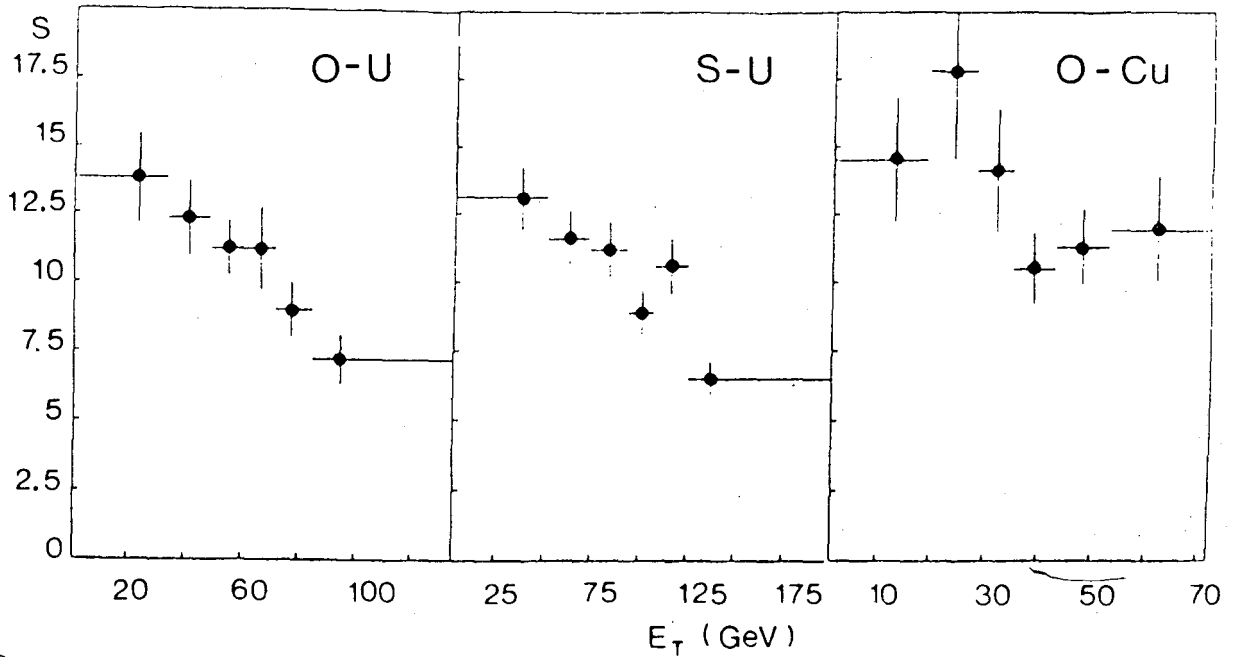
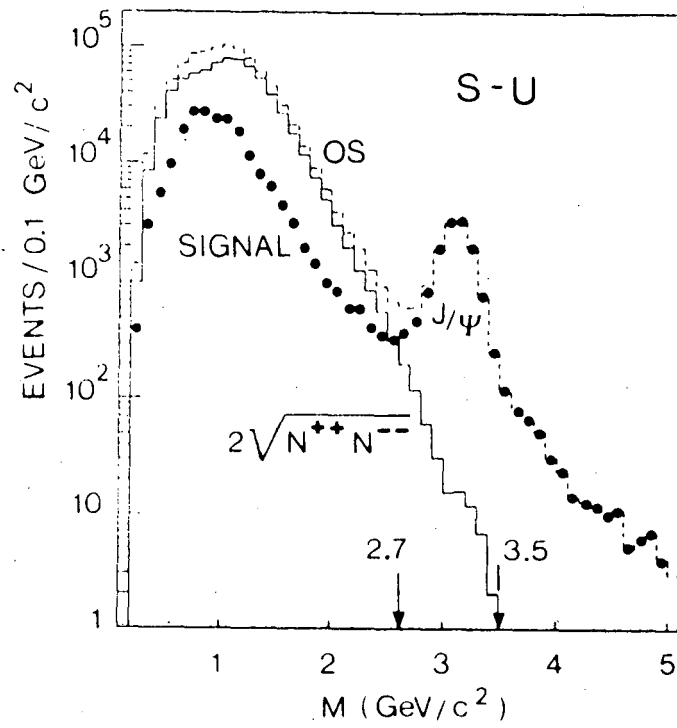


Fig.9

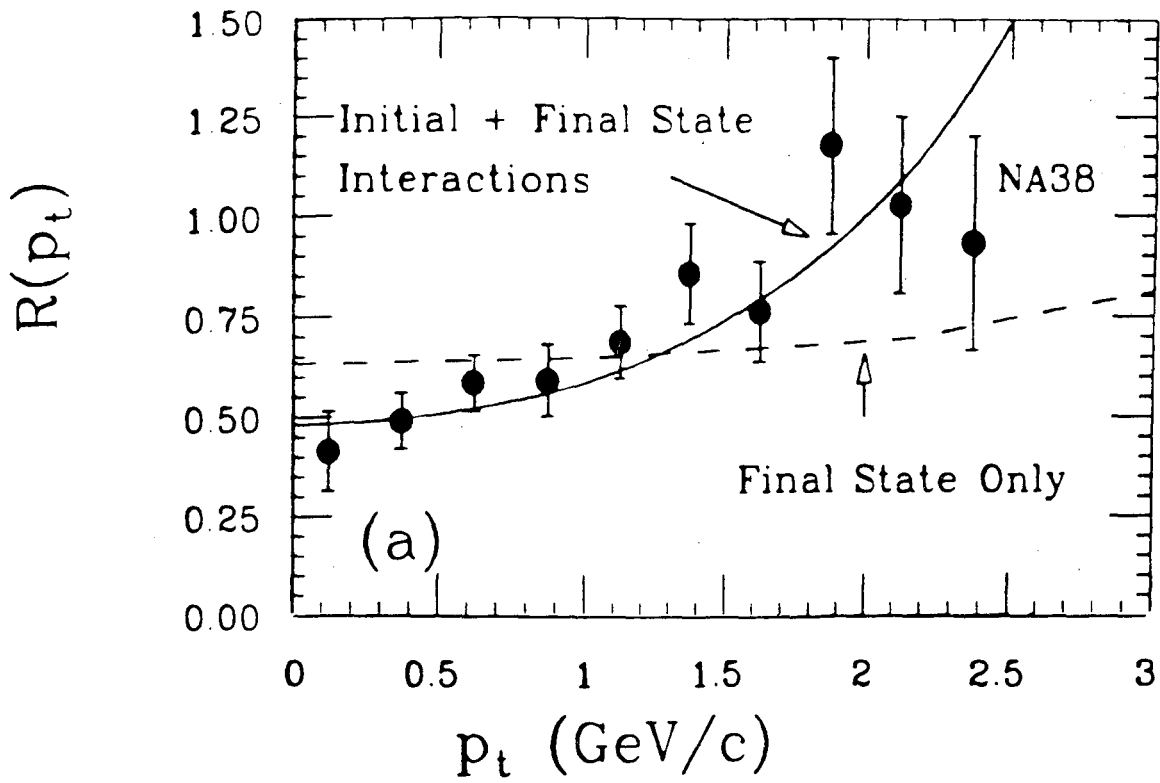


Fig.10

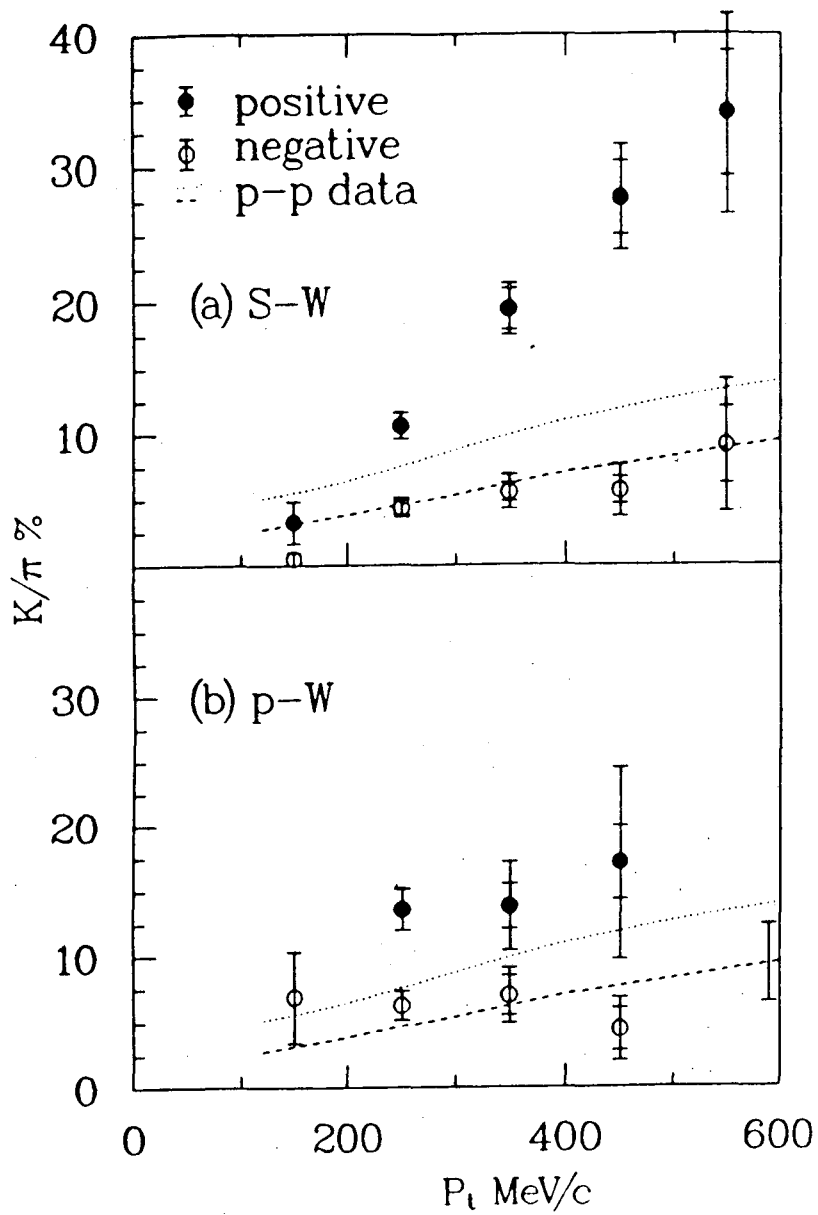


Fig.11

200 GeV/nucleon $S + S \rightarrow \Lambda + \text{anything}$

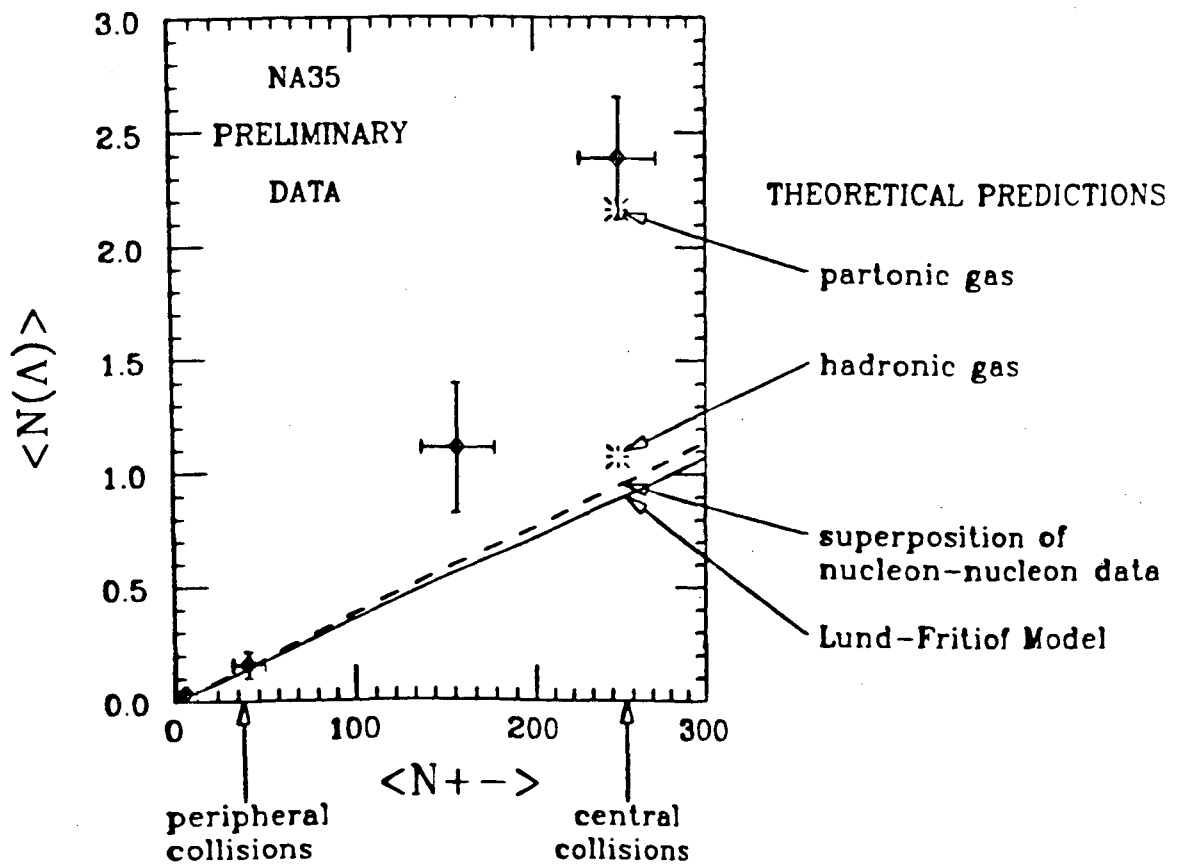


Fig.12

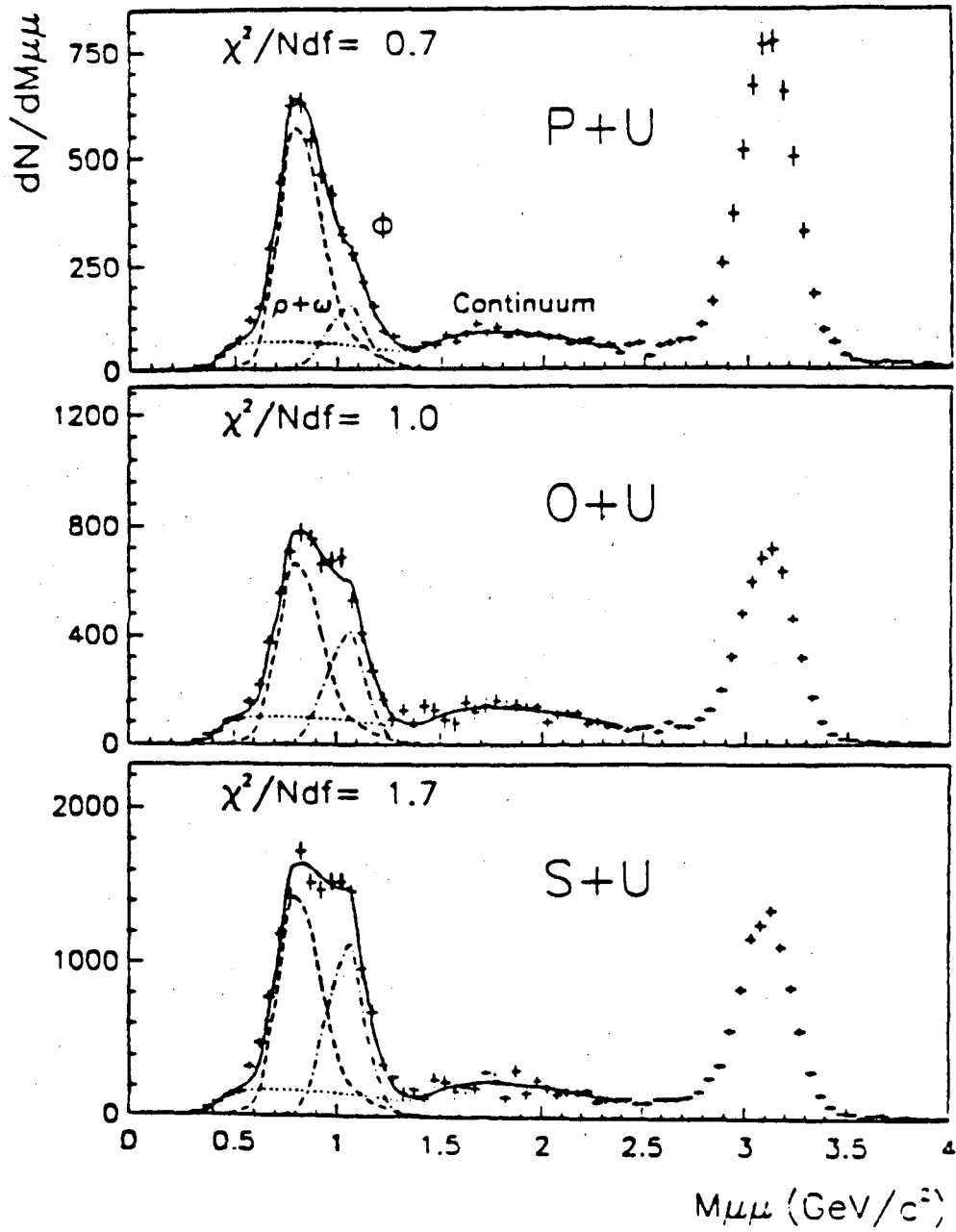


Fig.13

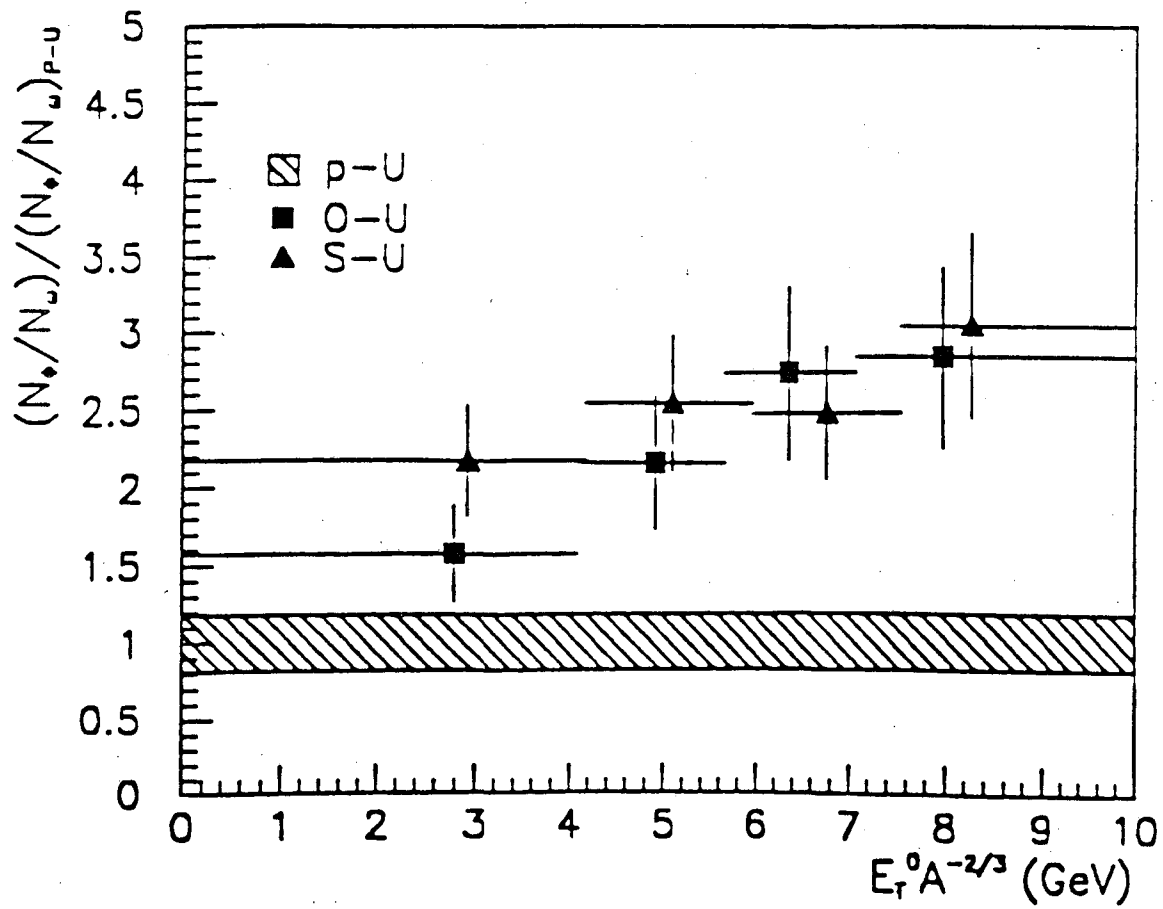


Fig.14

LAWRENCE BERKELEY LABORATORY
UNIVERSITY OF CALIFORNIA
INFORMATION RESOURCES DEPARTMENT
BERKELEY, CALIFORNIA 94720